RESEARCH PAPER

A quantitative model of amphetamine action on the 5-HT transporter

Walter Sandtner*, Diethart Schmid*, Klaus Schicker*, Klaus Gerstbrein, Xaver Koenig, Felix P Mayer, Stefan Boehm, Michael Freissmuth and Harald H Sitte

Center of Physiology and Pharmacology, Medical University Vienna, Vienna, Austria

BACKGROUND AND PURPOSE

Amphetamines bind to the plasmalemmal transporters for the monoamines dopamine (DAT), noradrenaline (NET) and 5-HT (SERT); influx of amphetamine leads to efflux of substrates. Various models have been proposed to account for this amphetamine-induced reverse transport in mechanistic terms. A most notable example is the molecular stent hypothesis, which posits a special amphetamine-induced conformation that is not likely in alternative access models of transport. The current study was designed to evaluate the explanatory power of these models and the molecular stent hypothesis.

EXPERIMENTAL APPROACH

Xenopus laevis oocytes and HEK293 cells expressing human (h) SERT were voltage-clamped and exposed to 5-HT, p-chloroamphetamine (*p*CA) or methylenedioxyamphetamine (MDMA).

KEY RESULTS

In contrast to the currents induced by 5-HT, *p*CA-triggered currents through SERT decayed slowly in *Xenopus laevis* oocytes once the agonist was removed (consistent with the molecular stent hypothesis). However, when SERT was expressed in HEK293 cells, currents induced by 3 or 100 μM *p*CA decayed 10 or 100 times faster, respectively, after *p*CA removal.

CONCLUSIONS AND IMPLICATIONS

This discrepancy in decay rates is inconsistent with the molecular stent hypothesis. In contrast, a multistate version of the alternative access model accounts for all the observations and reproduces the kinetic parameters extracted from the electrophysiological recordings. A crucial feature that explains the action of amphetamines is their lipophilic nature, which allows for rapid diffusion through the membrane.

Abbreviations

DAT, dopamine transporter; MDMA, methylenedioxyamphetamine; *p*CA, p-chloroamphetamine; SERT, 5-HT transporter

Introduction

Amphetamine and its congeners act on the three closely related plasmalemmal monoamine transporters, that is the transporters for dopamine (DAT), noradrenaline (NET) and 5-HT (SERT) (Kristensen *et al*., 2011). The individual amphetamine-derived compounds differ in their affinity for specific transporters but their principal mechanism of action is identical: they bind to the outward facing conformation of the transporter and translocate together with Na^+ and Cl^- from the extracellular side into the cell interior (Rudnick and Wall, 1992; Sitte *et al*., 1998; Seidel *et al*., 2005).

Amphetamines induce substrate efflux (Rothman and Baumann, 2003; Hilber *et al*., 2005; Baumann *et al*., 2012) and most if not all of their biological actions are due to their ability to raise the extracellular levels of dopamine, NA and 5-HT. Increased monoamine efflux by amphetamines is caused by a combination of effects and not all of them occur

at the level of the monoamine transporters; that is it is known that amphetamines increase cytosolic monoamine concentrations by the depletion of storage vesicles (Sulzer *et al.*, 1993). The elevated cytosolic concentrations of monoamines are then thought to enhance the outwardly directed substrate flux through SERT, DAT or NET (Sulzer *et al.*, 1995). Amphetamine-induced release is also known to be regulated by PKC and CaM-kinase-dependent phosphorylation (Gnegy, 2003; Seidel *et al.*, 2005; Fog *et al.*, 2006; Steinkellner *et al.*, 2012). Phosphorylation of intracellular portions of the transporter is likely to affect the rate at which the transporter moves from the inward to the outward conformation. In fact, mutations within the N-terminus shift the transporter into the inward-facing conformation and hamper amphetamine-induced substrate efflux (Sucic *et al.*, 2010). Several studies have proposed that amphetamines enhance and stabilize transporter conformations that are not induced by the native substrates (Petersen and DeFelice, 1999; Kahlig *et al.*, 2005). A recent report described an (S+)-amphetamine-specific leak current observed in *Xenopus laevis* oocytes expressing DAT (Rodriguez-Menchaca *et al.*, 2012). This current displayed peculiar features: it was induced by extracellular (S+)-amphetamine, but it did not require its continuous presence. In fact, it stayed activated long after (S+)-amphetamine had been removed from the solution, implying a long-lasting conformational change induced by amphetamine. DeFelice and coworkers termed this current a 'shelf current' and proposed a molecular stent hypothesis for amphetamine action, which invoked this persistent conductance as the pathway for efflux of accumulated substrate. Here, we observed that p-chloroamphetamine (*p*CA) induces SERT currents similar to the 'shelf currents' of (S+)-amphetamine-stimulated DAT. However, we showed that novel activities or conformational states of SERT are not required for these *p*CA-induced 'shelf currents' and that a recently established alternative access model (Schicker *et al.*, 2011; Bulling *et al.*, 2012) can adequately describe the action of *p*CA. Our observations suggest that *p*CA-induced 'shelf currents' are substrate-induced currents similar to those observed and described by other groups (Mager *et al.*, 1994; Quick, 2003; Erreger *et al.*, 2008). The reason that *p*CA-induced currents can appear to differ from currents triggered by 5-HT can be accounted for by the lipophilic nature of *p*CA.

Methods

cRNA preparation

Plasmids encoding hSERT were linearized and transcribed into RNA with a T7 RNA polymerase Kit mMessage mMachine (Ambion, Foster City, CA, USA). A total of 5 ng cRNA was microinjected into each oocyte. Electrophysiological recordings were performed 6–9 days following injection.

Oocyte preparation

Xenopus laevis frogs (Nasco, Fort Atkinson, WI, USA) were anaesthetized with ethyl 3-aminobenzoate methanesulfonate (FLUKA A5040, Sigma Aldrich, Seelze, Germany) 2 mg mL^{-1} in H$_2$O before the frogs were decapitated and the ovarian lobes removed and transferred to sterile Ca^{2+}-free OR2 solution (82.5 mM NaCl, 2.5 mM KCl, 2 mM MgCl$_2$, 10 mM HEPES, pH adjusted to 7.4 with NaOH). The lobes were manually dissected to produce groups of 5–10 oocytes and incubated in OR2, containing 1 mg mL^{-1} collagenase from *Clostridium histolyticum* (SIGMA, Sigma Aldrich). Forty-five to 60 min of incubation at 18°C were sufficient to digest and remove the follicular layer. Oocytes were then selected and transferred to a Ringer solution (100 mM NaCl, 2 mM KCl, 1.8 mM CaCl$_2$, 1 mM MgCl$_2$, 5 mM HEPES, pH adjusted to 7.6 with NaOH). Oocytes were kept at 18°C for a minimum of 2 h prior to injection. Injected oocytes were kept for 6–9 days at 18°C in a Ringer solution containing 2.5 mM Na+ pyruvate, 100 µg mL^{-1} penicillin, 100 µg mL^{-1} streptomycin. Solutions were changed daily.

Electrophysiological recordings in Xenopus laevis *oocytes*

A CA-1B high performance oocyte clamp (Dagan Corporation, Minneapolis, MN, USA) was employed for the measurements. The recorded signal was digitized with a Digidata 13222A (Axon Instruments, Sunnyvale, CA, USA). An Intel personal computer running pCLAMP 9.2 (Axon Instruments) was used for acquisition. Borosilicate glass capillaries were pulled to a final resistance of 0.4–1.2 MΩ and filled with 3 M KCl. Oocytes were impaled and the membrane potential was clamped to a holding potential of –60 mV. For continuous superfusion with ND100 solution (100 mM NaCl, 2 mM KCl, 1 mm CaCl$_2$, 1 mM MgCl$_2$, 10 mM HEPES, pH adjusted to 7.4 with NaOH), a gravity-driven superfusion system [Warner Instruments (Hamden, CT, USA), Eight Channel Perfusion Valve Control System (VC-8)] was used. Recordings were started after a stable current baseline had been established. The current was sampled with 100 Hz and low pass filtered with 20 Hz.

Whole-cell patch clamp

For patch clamp recordings, HEK293 cells stably expressing hSERT (Hilber *et al.*, 2005) were seeded at low density for 24 h before measuring currents. To measure substrate-induced hSERT currents, cells were voltage clamped using the whole-cell patch clamp technique. Briefly, glass pipettes were filled with a solution consisting of 133 mM K-gluconate, 5.9 mM NaCl, 1 mM CaCl$_2$, 0.7 mM MgCl$_2$, 10 mM EGTA and 10 mM HEPES adjusted to pH 7.2 with KOH. For some experiments, the internal K$^+$ concentration had to be reduced. In these instances, the pipette solution consisted of (mM) NMDG (163), MES (137), NaCl (5.9), CaCl$_2$ (1), MgCl$_2$ (0.7), HEPES (10), EGTA (10) pH 7.2.

The cells were continuously superfused with external solution 140 mM NaCl, 3 mM KCl, 2.5 mM CaCl$_2$, 2 mM MgCl$_2$, 20 mM glucose and 10 mM HEPES adjusted to pH 7.4 with NaOH. Currents were recorded at room temperature (20–24°C) using an Axopatch 200B amplifier and pClamp 10.2 software (MDS Analytical Technologies, Sunnyvale, CA, USA). Unless otherwise stated, cells were voltage clamped to a holding potential of –70 mV and 5-HT or *p*CA was applied for 5 s once every 60 s. Current traces were filtered at 1 kHz and digitized at 2 kHz using a Digidata 1320A (MDS Analytical Technologies). The liquid junction potential was calculated to be +16 mV and measurements were accordingly compensated. Drugs were applied using a DAD- 12 (Adams & List, Westbury, NY, USA), which permits complete solution exchange around the cells within 100 ms (Boehm, 1999). Current amplitudes in response

to 5-HT application were quantified using Clampfit 10.2 software (Axon Instruments). Passive holding currents were subtracted and the traces were filtered using a 100 Hz digital Gaussian low pass filter.

Quantitative pCA measurements

Diffusion of pCA into uninjected *Xenopus laevis* oocytes was determined by adapting the method developed from measuring uptake of amphetamines into HEK293 cells (Seidel *et al.*, 2005) as follows: single oocytes were incubated at room temperature in 1 mL ND100 solution containing 100 µM pCA. The respective incubation periods were 8, 16, 32, 64 128, 256 or 600 s. After incubation in pCA, the cells were transferred into 10 mL of a pCA free ND-100 solution and washed for 3 to 5 s. The oocytes were then transferred to an Eppendorf reaction tube. The carry-over of wash solution was about 20 µL. The sample was spiked with internal standard (50 ng of amphetamine) and pCA was extracted from the cell by addition of acetonitrile (0.25 mL). After centrifugation, the supernatant (0.15 mL) was mixed with an equal volume of aqueous solution (pH 9.2; final concentration, 15 mM Na_2HPO4) containing dansyl chloride (6.25 µg, Serva Feinbiochemika, Heidelberg, Germany). After 20 min at 65°C, the samples were centrifuged to remove precipitated material; 0.15 mL were injected into an HPLC system and resolved at a flow rate of 1 mL min^{-1} at 50°C (mobile phase, 1:1; 30 mM KH2PO4, pH 6;.acetonitrile; column, Hewlett-Packard Hypersil MOS 200 _ 2.1 mm (Thermo Fisher Scientific Inc., Waltham, MA, USA); fluorescence detection, Shimadzu RF-551 Shimadzu, Kyōto, Japan; excitation and emission wavelength, 318 and 510 nm respectively).

Modelling

We modelled the recorded currents utilizing a previously published kinetic model of the transport cycle of SERT. The time-dependent changes in state occupancies were evaluated by numerical integration of the resulting system of differential equations using Systems Biology Toolbox (Schmidt and Jirstrand, 2006) and MATLAB 2012a (Mathworks, Natick, MA, USA).

The voltage-dependence of individual rates was modelled according to Laeuger (1991) assuming a symmetric barrier as $k_{ij} = k0_{ij}exp(-zQ_{ij}FV/2RT)$, with F = 96 485 $Cmol^{-1}$, R = 8.314 $JK^{-1} mol^{-1}$ and V the membrane voltage in volts and T = 293 K. The uncoupled current was modelled as a current through a Na^+ permeable channel with I = $Pc\gamma NC(V-V_{rev})$, with Pc being the occupancy of the channel state, γ the single channel conductance of 2.4 pS (Lin *et al.*, 1996), NC the number of channels, V the membrane voltage and V_{rev} the reversal potential of Na^+ being +80 mV. The extra- and intracellular ion concentrations were set to the values used in the experiments. Extra- and intracellular substrate concentrations at the membrane interfaces – S_{out} (t) and S_{in} (t) – were modelled as described in the supplement.

Statistics

All values are given as mean ± SD. The statistical significance of differences between groups was analysed using Mann–Whitney U-test. P-values <0.05 were considered to indicate statistical significance.

Results

Assessment of pCA-induced currents in Xenopus laevis *oocytes expressing hSERT*

The deactivation of pCA-induced currents occurs more slowly than the deactivation of currents induced by the native substrate (5-HT). Figure 1A and B show representative current traces
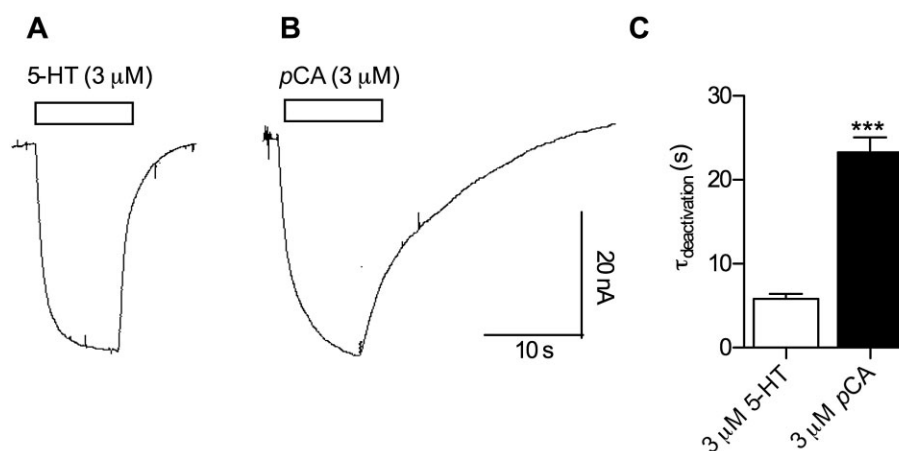
Figure 1

Differences between currents induced by 5-HT and pCA respectively. *Xenopus laevis* oocytes expressing hSERT were clamped to −60 mV. Currents induced by 3 µM 5-HT were compared with currents from the same cell induced by 3 µM pCA. (A) 3 µM 5-HT was applied to the cell for 10 s and subsequently washed away with a gravity driven perfusion system. (B) The same procedure was repeated with 3 µM pCA. (C) The current decays were fitted to mono-exponential functions and the time constants were plotted in the bar graph. A comparison of the decay time constants following 5-HT (5.8 s ± 1.3 s, n = 6) and pCA removal (23.3 s ± 4 s, n = 6) revealed a significantly slower time constant for pCA (*** = P < 0.001, Mann–Whitney U-test).

recorded in *Xenopus laevis* oocytes expressing hSERT, measured using the two-electrode voltage clamp technique. The membrane voltage was clamped to –60 mV and 3 μM 5-HT was applied to the cell (Figure 1A); 5-HT provoked an inwardly directed current that reached a steady amplitude during the exposure time (10 s). Upon 5-HT removal, the current decayed exponentially to the initial level with a time constant of 5 s (this process is referred to as deactivation throughout the subsequent description). A current of similar size was induced when the same cell was challenged with 3 μM *p*CA (Figure 1B). However, after removal of *p*CA, the current deactivated about four times slower with a time constant of ~20 s (Figure 1C).

The current amplitudes as a function of increasing 5-HT/pCA concentrations. *Xenopus laevis* oocytes clamped to a holding potential of –60 mV were challenged with increasing concentrations of *p*CA (Figure 2B). Application of lower concentrations (up to 10 μM) led to an increase in the measured current while higher concentrations led to inhibition. This is reflected in the bell-shaped concentration-response curve plotted in Figure 2A (closed circles). A concentration ramp of 5-HT (Figure 2A, open circles) was also associated with a reduction in current at higher concentrations; however, the inhibitory effect was less pronounced in the concentration range from 100 μM to 1 mM. These data show that *p*CA and 5-HT exert two effects on SERT: activation of a current at low
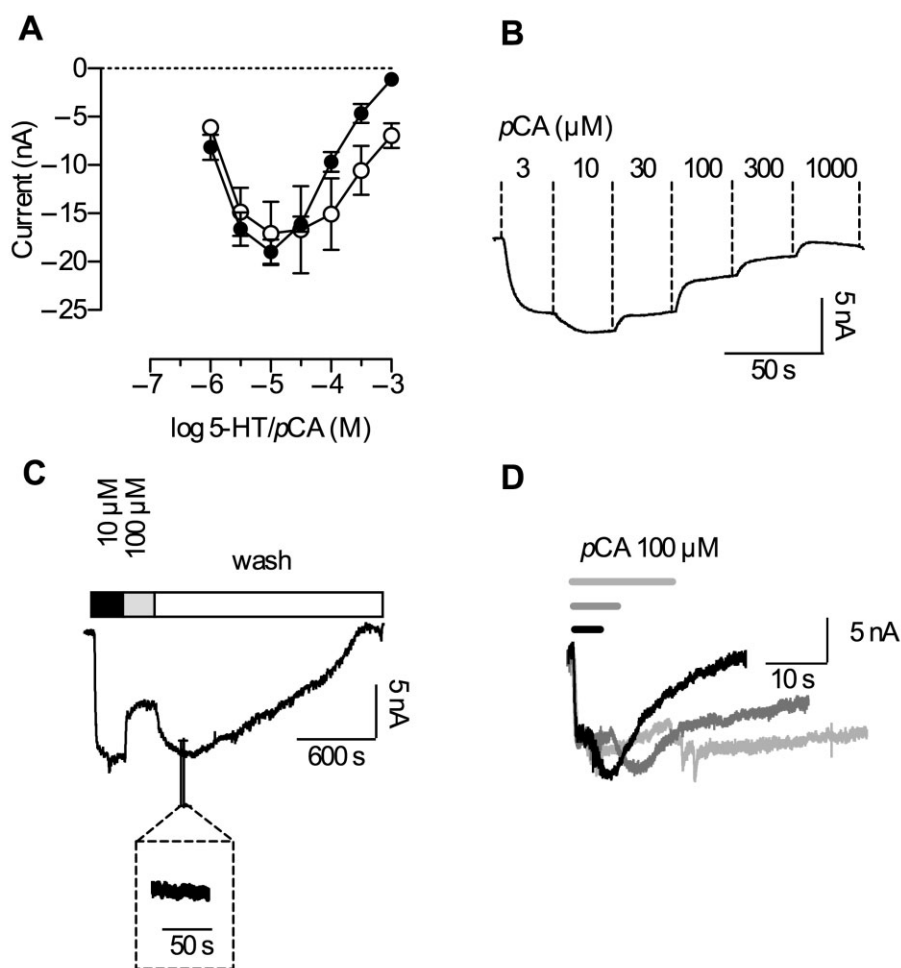
Figure 2

Concentration-dependence of currents induced by 5-HT and *p*CA. Single *Xenopus laevis* oocytes were voltage clamped to –60 mV using the two electrode voltage clamp technique. Cells were continuously superfused with buffer solution. For the evaluation of the current amplitudes, the cells were either challenged with increasing concentrations of 5-HT or *p*CA. (A) The currents induced were recorded for both substrates ($n = 5$ each), averaged and plotted as a function of increasing 5-HT/*p*CA concentrations with lines connecting the data points. *p*CA (closed circles) and 5-HT (open circles) stimulation led to similar maximal current amplitudes; however, the inhibitory effect of *p*CA was more pronounced, as indicated by a stronger current suppression at high concentrations. (B) A representative experiment illustrating current responses to increasing *p*CA concentrations. The current exhibited a maximum at 10 μM *p*CA and was fully suppressed at 1 mM. (C) A representative current trace recorded at –60 mV; 10 μM *p*CA elicited the maximal current amplitude whereas 100 μM *p*CA inhibited the current partially. After removal of *p*CA, the current initially rose to a higher level; 30 to 40 min were required for its full decay (the inset shows a magnification of the current trace). Hence, the current appears to be persistent when monitored at the time scale indicated (10 to 100 s). (D) Prolonged exposure to *p*CA leads to slowed deactivation; currents elicited by 100 μM *p*CA are shown. The respective exposure times were 4 (black), 8 (dark grey) and 16 s (light grey).

and inhibition at higher concentrations. However, *p*CA was more potent at inhibiting the current.

'Persistent' current after removal of high p*CA concentrations.* DeFelice and coworkers observed a persistent current through DAT expressed in *Xenopus laevis* oocytes, when they challenged the transporter with (S+)-amphetamine and then removed (S+)-amphetamine from the solution. (S+)-amphetamine concentrations above 10 μM had to be applied to evoke this current. Here, we tested if SERT would also conduct a persistent current when challenged with *p*CA in a similar concentration range. A representative current trace is depicted in Figure 2C: The maximal current amplitude was induced by 10 μM *p*CA, followed by the application of 100 μM *p*CA. The current amplitude decreased in agreement with the concentration-response relation shown in Figure 2A. Upon removal of *p*CA, the current amplitude increased again, reaching a level comparable to that seen in the presence of 10 μM *p*CA. Thereafter, the current decayed slowly over 30 to 40 min. We stress that this decay was not observed when currents were monitored within a narrower time window, that is over a time scale of 10 to 100 s as is commonly used in most other studies of transporter-associated currents (Mager *et al*., 1994; Adams and DeFelice, 2003; Quick, 2003). In this narrower time range, the current appears to be persistent (Figure 2C, inset). DeFelice and coworkers showed that the 'persistent' current invoked by the removal of (S+)-amphetamine in DAT increased upon prolongation of the exposure to (S+)-amphetamine. In SERT, similar to DAT, the current contingent on *p*CA removal also changed in a time-dependent manner (Rodriguez-Menchaca *et al*., 2012). Figure 2D shows representative current traces that were recorded after different exposure times (i.e. after 4, 8 and 16 s). The applied *p*CA concentration was 100 μM in all instances. However, upon prolonged administration, *p*CA gave rise to currents that lasted longer.

Assessment of p*CA-induced current properties in HEK293 cells expressing SERT.* The data shown in Figures 1 and 2 were recorded from *Xenopus laevis* oocytes injected with SERT cRNA. We also recorded *p*CA- and 5-HT-induced currents in HEK293 cells stably expressing hSERT using patch clamp recordings in the whole cell configuration. As shown in Figure 3A (lower trace) 3 μM *p*CA induced an inwardly directed current in HEK293 cells clamped to –70 mV. Similar to the observation in oocytes, removal of *p*CA led to slow deactivation of the current. In further agreement with the recordings in oocytes, the time constant for 3 μM *p*CA was about five times slower than for 3 μM 5-HT (Figure 3A, upper trace). However, we also identified important differences. The most notable was found for the time course of current deactivation upon *p*CA removal: while the current decays were well described by a mono-exponential function in both HEK293 cells and *Xenopus laevis* oocytes, the absolute values of the time constants differed by ~10-fold (compare Figures 1C and 3B).

Lack of 'persistent currents' upon removal of high concentrations of p*CA in HEK293 cells.* The kinetics of currents measured in HEK293 cells upon application of high *p*CA concentrations (>10 μM) differed substantially from those recorded in
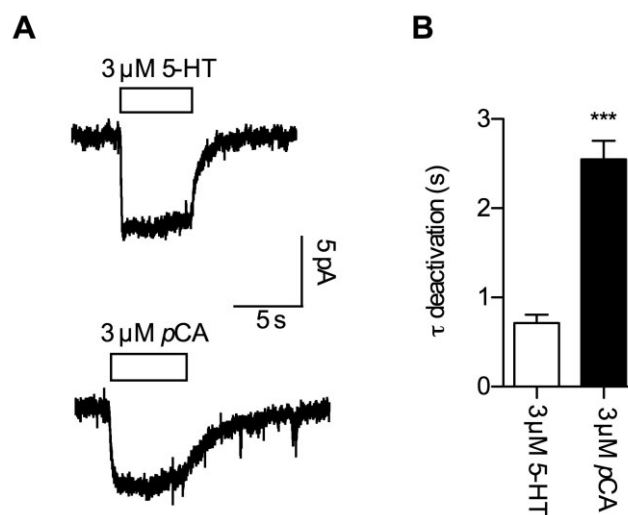
Figure 3

Comparison of current responses to 5-HT and *p*CA in HEK293 cells expressing SERT. Cells were continuously perfused with buffer and voltage clamped to –70 mV utilizing the whole cell patch clamp technique. (A) Inwardly directed currents provoked by 3 μM 5-HT (upper trace) or 3 μM *p*CA (lower trace); 5-HT/*p*CA were applied for 5 s and then removed from the solution utilizing a fast perfusion system (see experimental procedures). (B) Current deactivation upon removal of 5-HT and *p*CA was fitted to a mono-exponential function and the time constants derived were plotted in a bar graph. Comparison of the decay time constants following 5-HT removal (0.712 s ± 0.094 s, $n = 9$) and *p*CA removal (2.549 s ± 0.208 s, $n = 9$) reveals a significantly slower time constant for *p*CA (*** = $P < 0.001$, Mann–Whitney U-test).

Xenopus laevis oocytes. While the latter exhibited only a steady current partially reduced by concentrations above 10 μM *p*CA (Figure 2B,C), currents measured in HEK293 cells upon application of high *p*CA concentrations were transient, as depicted in Figure 4A. After a brief initial peak, the current inactivated during a 5 s application of *p*CA and reached baseline values in the case of 100 μM. The time course of inactivation was fitted to a mono-exponential function, which yielded a time constant of about 230 ms at 100 μM *p*CA. It is important to note and it will be shown later that this transient component is different from the capacitive current previously described (Schicker *et al*., 2011). When current amplitudes were measured at the end of a 5 s exposure to different *p*CA concentrations, the resulting plots recapitulated the bell-shaped concentration-response curves found in *Xenopus laevis* oocytes (Figure 2A). We surmise that the lack of the transient component in *Xenopus laevis* oocytes was due to the slow solution exchange rates that can be achieved upon superfusion of oocytes; because of the large volume, wash-in of compounds is slow and rate-limiting. In contrast, solution exchange is rapid in patch clamp experiments with HEK293 cells allowing for superior time-resolved recordings. Recapitulating the findings in *Xenopus laevis* oocytes, the current showed an initial increase in amplitude upon removal of 30 μM or 100 μM *p*CA. However, following the initial peak, the current deactivated with a time constant of about 13 s
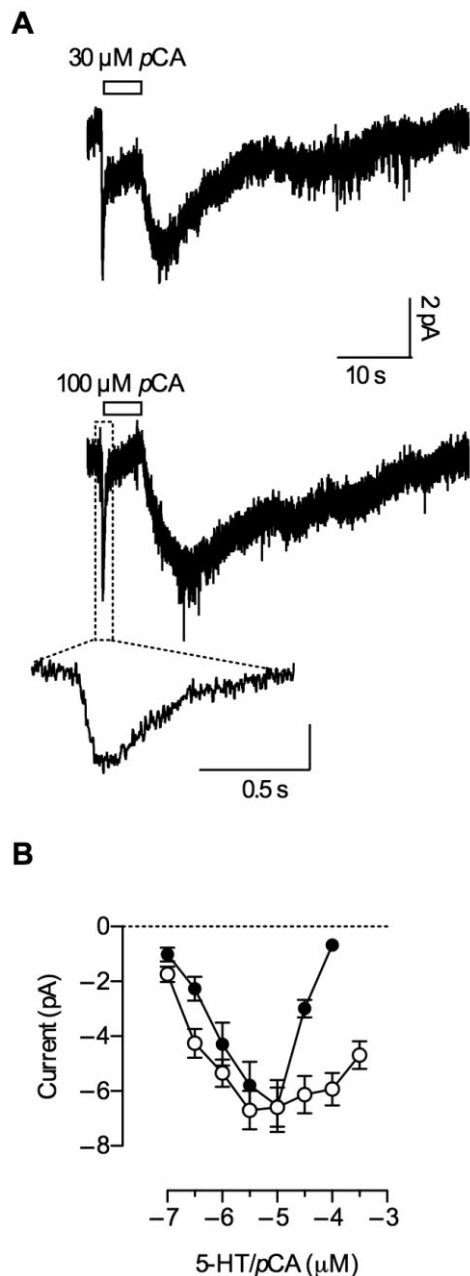
Figure 4

Current responses to high *p*CA concentrations in HEK293 cells. (A) Representative current traces recorded from HEK293 cells expressing hSERT induced by 30 and 100 μM *p*CA respectively. Cells were clamped to −70 mV and *p*CA was applied for 5 s, before it was removed from the solution. Exposure to 30 and 100 μM *p*CA resulted in an inwardly directed current that inactivated quickly during exposure (261 ms ± 70 ms, *n* = 8, and 223 ms ± 60 ms, *n* = 8, at 30 and 100 μM *p*CA respectively). The current first recovered and then deactivated after removal of *p*CA (7.8 s ± 2.5 s at 30 μM, *n* = 8, and 13.2 s ± 4.7 s, *n* = 8, at 100 μM *p*CA). The initial current peak on an expanded time scale is shown in an inset. (B) Current amplitudes upon stimulation by increasing 5-HT/*p*CA concentrations – measured after 5 s of exposure – were plotted as a function of concentration (*n* = 8 each) with lines connecting the data points. *p*CA (closed circles) and 5-HT (open circles) led to similar maximal current amplitudes; however, the inhibitory effect of *p*CA was more pronounced.

after removal of 100 μM *p*CA. In contrast, as shown above, in oocytes the current decayed fully only after 30 to 40 min. This discrepancy is too large to be attributed to different solution exchange times. These data show that *p*CA did not induce persistent currents in HEK293 cells.

pCA-induced currents require internal K⁺.   In a recent study, we demonstrated that 5-HT-induced currents through SERT are comprised of two components: utilizing a fast perfusion device, we observed an inwardly directed current peak followed by a steady current when SERT was challenged with 5-HT (Schicker *et al.*, 2011). In the same study, we showed that removal of internal K^+ suppressed the steady current but left the peak current unchanged. In the current study, we determined whether *p*CA-induced currents are similarly affected by the absence of internal K^+. Figure 5 shows a representative current trace from a HEK293 cell clamped to −70 mV. At 100 μM, *p*CA elicited a peak current very similar to that previously observed with 5-HT (Schicker *et al.*, 2011). This contrasts with the recording shown in Figure 4A (lower trace) where the same *p*CA concentration was applied but the intracellular solution in the patch electrode contained 164 mM K^+. The comparison shows that *p*CA-induced currents were fully suppressed in the absence of K^+, including the slowly deactivating current that had followed *p*CA removal. The peak current decayed with a time constant of about 70 ms (see inset Figure 5). This is considerably faster than the transient current shown in Figure 4A. Taken together, these data are consistent with the hypothesis that *p*CA- and 5-HT-induced currents are carried by the same conducting state.

Current inhibition at higher substrate concentrations is a consequence of internal substrate accumulation.   In the original description of SERT-associated currents, Lester and coworkers observed current inhibition at external 5-HT concentrations exceeding 3 μM, but the underlying mechanism has remained elusive. In the present study, we addressed the mechanistic basis for this action of 5-HT. In principle, two mechanisms can be envisaged that result in decrease in current amplitude. The first encompasses a direct block of the conducting state by the substrate. This mechanism implies the presence of a second substrate-binding site of low affinity within the conduction pathway. The model posits that occupation of this site with substrate causes the current block. An alternative model assumes a change in the conformational equilibrium by internally accumulating substrate. This results in a reduced dwell time of SERT in the conducting state, because high internal substrate concentrations favour re-association of substrate to the internal substrate-binding site and thus impede progression through the transport cycle. Thus, by definition, high internal substrate alters the conformational equilibrium.

Figure 6A shows original traces of substrate currents induced at −70 mV by 30 and 100 μM methylenedioxyamphetamine (MDMA) respectively. MDMA induced a current that resembled the *p*CA current shown in Figure 4A. Similar to the *p*CA-induced current, the MDMA current first increased and then decreased rapidly reaching a new steady state within the application time (5 s). Similarly, application of 100 μM 5-HT also resulted in a current run-down, which, however, emerged more slowly and hence required a longer
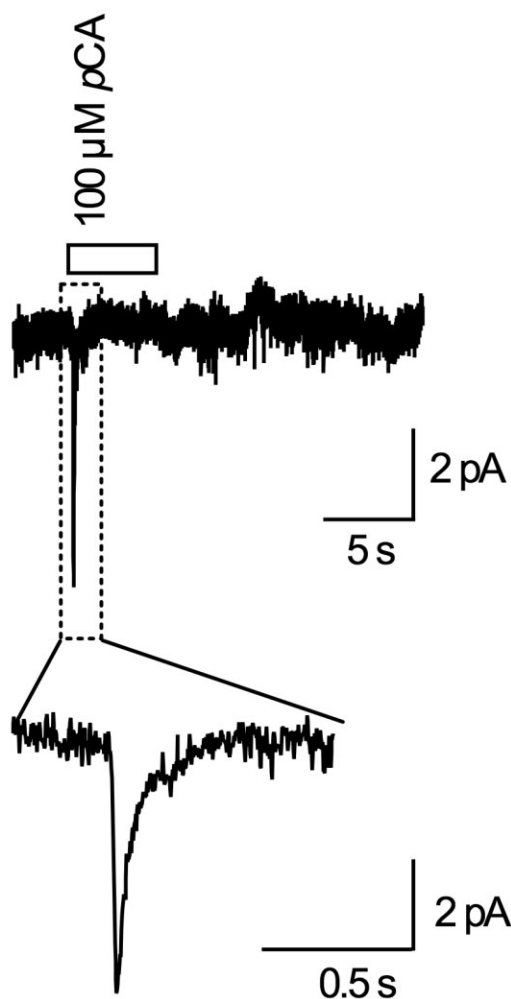
Figure 5

*p*CA-induced current in the absence of internal K$^+$. Representative current trace recorded from a HEK293 cell expressing hSERT clamped to −70 mV. Internal K$^+$ was replaced with NMDG$^+$ (see experimental procedures) and the cell was challenged with 100 μM *p*CA for 5 s with a fast perfusion device (see also experimental procedures). *p*CA evoked a fast current peak, but the steady current that also included the current following *p*CA removal is absent (compare with Figure 4A-lower trace). The peak current is shown in an inset with an expanded time scale. The current decay was well fitted by a mono-exponential function and the fit yielded a time constant of 70 ± 21 ms (*n* = 5); compare this with time constants from Figure 4.

steady state for increasing concentrations of 5-HT. The extracted IC$_{50}$ value around 100 μM are in good agreement with the IC$_{50}$ value for internal substrate block determined by DeFelice and coworkers and the K_M of 5-HT for the internal site (Sitte *et al.*, 2001; Adams and DeFelice, 2003). This again suggests that the observed current inhibition at high substrate concentrations is caused by internal substrate accumulation. The rapid onset of current inactivation in the case of amphetamines suggested that there was substantial diffusion-driven uptake of *p*CA into oocytes. We tested this conjecture by assessing *p*CA diffusion directly: we measured uptake of *p*CA by uninjected *Xenopus laevis* oocytes. Single *Xenopus laevis* oocytes were exposed to 100 μM *p*CA, after a brief wash, the *p*CA level that remained in the oocyte was determined (see methods). Figure 6E shows the plot of *p*CA accumulated per oocyte as a function of the exposure time. These data were adequately described by an equation for a mono-exponential rise to equilibrium. Based on the parameter estimates, we calculated an equilibration time constant of about 135 s. It is worth noting that the calculated diffusion time of freely diffusing *p*CA is around 170 s 500 μm^{-1}. Thus, given the diameter of an oocyte (500 to 1000 μm), the observations are consistent with the interpretation that the speed of equilibration is only limited by the velocity of free diffusion. Conversely, the findings also imply that the cell membrane does not impose a major diffusion barrier for *p*CA. These data are therefore again in agreement with the hypothesis that the rapid inactivation observed with *p*CA (see Figure 4A) is a consequence of amphetamine accumulation within the cell.

A model of SERT function in the presence of amphetamines. Recently, we established an alternative access model of SERT function that links transporter-associated currents to substrate translocation (Schicker *et al.*, 2011). In this model, activation of currents by external substrates is associated with the formation of a K$^+$ bound inward-facing conformation in equilibrium with the conducting state. The results of the present study suggest that, at high concentrations, external substrates exert inhibitory effects on the currents (Figures 2A, 4B). Although inhibition by extracellular substrates is not a feature of our model, current inhibition is predicted to occur at high internal substrate levels.

Upon inward transport, the internal substrate concentration is expected to rise over time. In previous studies (Schicker *et al.*, 2011; Bulling *et al.*, 2012), substrate application was modelled as a step function and the effect of internal substrate accumulation was ignored. However, in the case of amphetamines, concentrations of substrate on the cytoplasmic (S_{in}) and external (S_{out}) faces of the transporter are both expected to follow a complex time course, if passive diffusion through the membrane is taken into account. The respective substrate concentrations as a function of time [$S_{in}(t)$ and $S_{out}(t)$] are critical factors for emulating current responses in our SERT model.

Here, we tested the hypothesis that 5-HT and *p*CA interact with SERT in an identical fashion (all parameters of the transport model kept unchanged) and that the observed differences between substrates (5-HT and *p*CA) and between HEK293 cells and *Xenopus laevis* oocytes can be attributed to internal reservoirs of accumulated amphetamine. Addressing this hypothesis requires a plausible model to predict $S_{in}(t)$ and

application period to reach steady state (Figure 6B-lower trace). Figure 6C shows a semi-logarithmic plot of the time constant of current inactivation (at 100 μM) as a function of the polar surface area (PSA) of each compound. The PSA, a good predictor of membrane permeability, is proportional to the energy term in the exponential of the rate constant (Reynolds *et al.*, 1974; Baldwin, 2013). Thus, the observed linear relation in the semi-logarithmic presentation is consistent with the hypothesis that the current inactivation occurs as a consequence of substrate permeation into the cell. Figure 6D shows the unblocked fraction of 5-HT current at

Figure 6

Current inhibition is a consequence of internal substrate accumulation. (A) Representative currents recorded in HEK293 cells at −70 mV induced by 30 and 100 μM MDMA respectively. MDMA was applied for 5 s and then removed from the external solution. Similar to the *p*CA-induced current (compare Figure 4), the current inactivated rapidly within the application time. The extracted time constants were 930 ms ± 180 ms ($n = 5$) and 780 ms ± 150 ms ($n = 5$) for 30 and 100 μM MDMA respectively. (B) Currents induced by 30 and 100 μM 5-HT; 5-HT was applied for an extended time period (see scale bar). In the case of 100 μM 5-HT, the current reached a steady level at about 50% of the initial amplitude. The respective time constant for current inactivation was 32 s ± 11 s ($n = 6$). (C) The logarithm of the time constant for current inactivation ($\sigma_{inactivation}$) at 100 μM *p*CA, MDMA and 5-HT was plotted as a function of the polar surface area (PSA); these values were taken from chemicalize.org. (D) The ratios of the initial current amplitude and the steady current amplitude are plotted as a function of increasing 5-HT concentrations. Each data point is the average of six experiments. The average values were fitted to the following equation: Y = $1/(1 + 10 \wedge ((X - \log IC_{50})))$. The extracted IC_{50} was 131 μM [95% confidence interval: 83.36–207.8 μM]. (E) *p*CA uptake into uninjected *Xenopus laevis* oocytes. The level of accumulated *p*CA in pmol per oocyte is plotted as a function of the exposure time to *p*CA (100 μM). Each data point is the average of six experiments. The line indicates a fit to a mono-exponential function. The extracted time constant was 134 s [95% confidence interval: 83–345 s].

$S_{out}(t)$. Accordingly, we formulated a model that included the following elements: (i) substrate fluxes through transporters and membranes, (ii) an external compartment subject to diffusion (unstirred layer), (iii) a stirred external compartment with infinite volume, and (iv) internal reservoir compartments with a plausible volume. We arranged all these elements as depicted in the scheme shown in Figure 7A. Realistic parameters (see Supplement) were extracted from the literature and the resulting system of differential equations was solved numerically. Two examples are shown in Figure 7B and C. In Figure 7B, 100 μM 5-HT was applied *in silico* for 5 s to an assumed HEK293 cell expressing SERT. The respective concentrations – $S_{out}(t)$ and $S_{in}(t)$ – predicted by our model are displayed. $S_{out}(t)$ and $S_{in}(t)$, give rise to the simulated current response I(t). The second example (Figure 7C) assumes a 5 s application of 100 μM *p*CA. Here, the respective concentrations over time differ, because $S_{in}(t)$ ramps up faster to higher

concentrations; this occurs as a consequence of passive diffusion through the membrane. The time course of $S_{out}(t)$ and $S_{in}(t)$ depicted gives rise to the calculated response I(t). Emulated current responses predicted by the model are shown in Figure 7D, E, F, H and I. Figure 7G displays the predicted *p*CA uptake into an uninjected *Xenopus laevis* oocyte. It is evident that the simulations match the corresponding currents determined in oocytes and cells respectively (compare Figure 1A, Figure 1B, Figure 2C, Figure 4A and Figure 4C).

Discussion and conclusions

Various hypotheses have been put forward to account for the ability of amphetamines to trigger efflux through monoamine transporters. These models fall into two categories: the first is based on the original concept of exchange diffusion
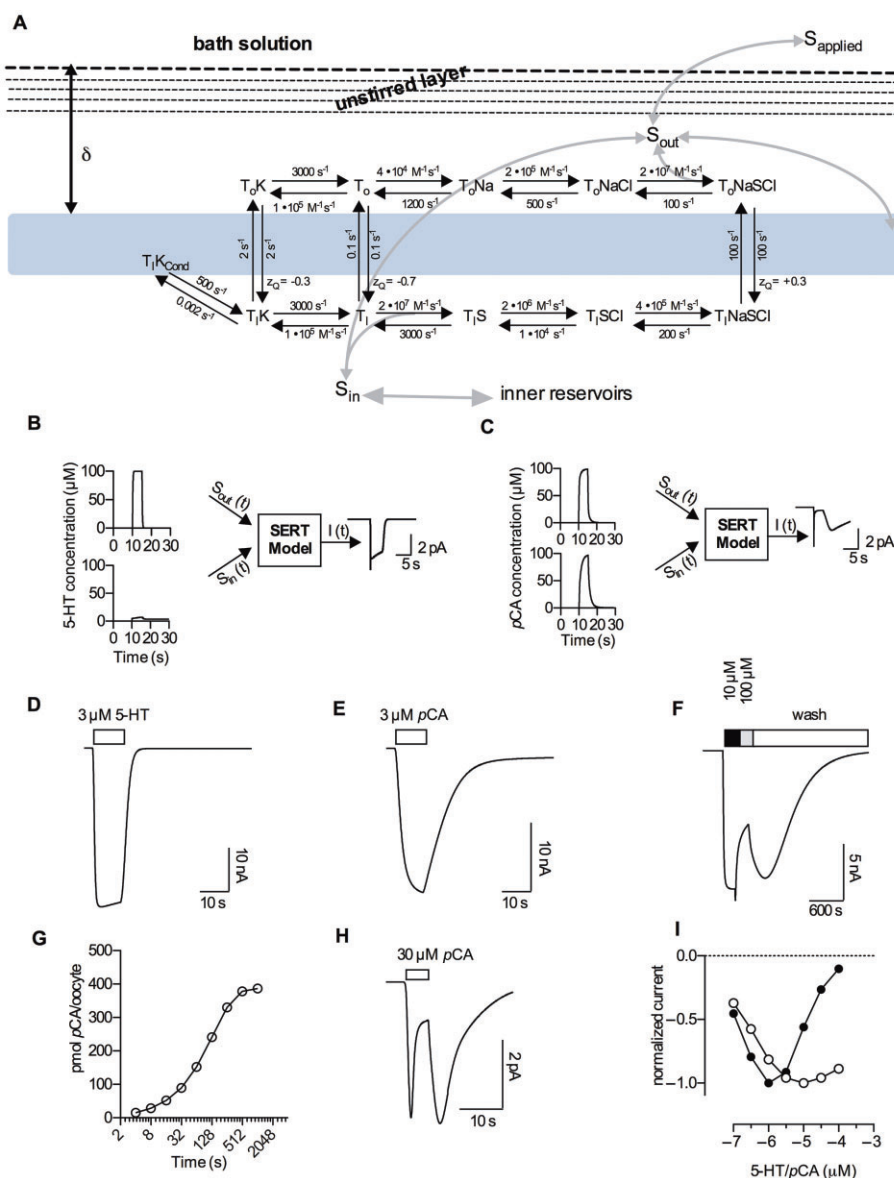
Figure 7

A model of amphetamine's action on SERT. (A) Alternative access model of SERT function in the presence of amphetamine, based on our previous findings. An unstirred solution layer surrounding the membrane at the width ∂ is included (the membrane is indicated as light blue rectangle). The unstirred solution layer was modelled by assuming five compartments separated by imaginary barriers. Grey arrows indicate substrate fluxes. (B) and (C) show examples of external and internal substrate concentrations as a function of time [S_{out} (t) and S_{in} (t)], as predicted by our model (see the model description in the supplement). I(t) is the calculated current produced by a given combination of S_{out} (t) and S_{in} (t). We assumed an application of 100 μM 5-HT in panel B and application of 100 μM pCA in panel C. Panels D–H show simulated current traces. (D) Calculated current induced by 3 μM 5-HT for SERT expressed in *Xenopus laevis* oocytes. (E) Calculated current induced by 3 μM pCA in oocytes. (F) Pseudo-persistent current following removal of 100 μM pCA, simulated for a *Xenopus laevis* oocyte expressing SERT. (G) Simulated pCA uptake into a single uninjected *Xenopus laevis* oocyte. (H) Simulated SERT current from HEK293 cells challenged with 30 μM pCA. (I) Simulated current amplitudes as a function of concentration measured after 5 s for 5-HT (open circles) and pCA (closed circles). This calculation was conducted for HEK293 cells expressing SERT; the calculated data points were connected with lines.

(Fischer and Cho, 1979) and include variations that focus on the oligomeric arrangement of the transporter to explain transporter-mediated efflux (Seidel *et al.*, 2005; Sitte and Freissmuth, 2010; Sucic *et al.*, 2010). The alternative approach focuses on the capacity of amphetamines to induce channel-like activity in transporters (Sonders *et al.*, 1997;

Sitte *et al.*, 1998; Kahlig *et al.*, 2005). The recently proposed molecular stent hypothesis is an extension of the latter models (Rodriguez-Menchaca *et al.*, 2012): it assumes the presence of a second binding site within the inner vestibule of the transporter. This site cannot be occupied by the cognate substrate but only by amphetamines, which were

proposed to induce a long-lasting channel-like mode in the transporter. The principal argument in favour of this model was the observation of a long-lasting amphetamine-induced current (termed 'shelf current') through DAT that persisted after removal of extracellular amphetamine.

Here, we examined several predictions of these models on SERT. We also observed a long-lasting current through SERT that was seen only upon superfusion with pCA, but not with 5-HT. However, the decay kinetics depended on the nature of the cell in which the transporter was expressed. Upon removal of 100 μM pCA, the current disappeared 100 times more rapidly in HEK293 cells than in *Xenopus laevis* oocytes. The molecular stent hypothesis predicts that the deactivation kinetics are an intrinsic feature of the amphetamine binding site at the inner gate of the transporter rather than a property conferred onto the transporter by the cellular context.

In line with earlier observations (Gobbi *et al.*, 2008), we observed a bell-shaped concentration-response curve: concentrations of pCA exceeding 10 μM resulted in progressively smaller currents. Furthermore, when pCA was completely removed from the bath solution, the current re-emerged. These observations are also difficult to reconcile with the core tenet of the molecular stent hypothesis, that is an amphetamine binding site at the inner gate. While our findings are not easily explained by the molecular stent hypothesis, they are consistent with an alternative access model.

Transporter-associated currents are a very sensitive readout because they allow for high temporal resolution. Accordingly, they monitor conformational changes in the transporter in real time. However, until recently, it was not clear how to understand the SERT-associated currents in the context of an alternative access model of substrate translocation. We identified the conformational state that gives rise to transport-associated currents and developed a mathematical model that provides a plausible kinetic description of SERT catalytic cycle (Schicker *et al.*, 2011). In the inward-facing (K$^+$-bound) conformation, SERT can apparently adopt a conducting state (T$_I$K$_{cond}$ in Figure 7A). Monitoring the current thus allows for estimating the abundance of T$_I$K$_{cond}$.

Both pCA and 5-HT can enter into cells by passive diffusion. However, because of its lipophilicity, pCA (PSA = 26.02 Å^2) diffuses across the membrane much faster than the more hydrophilic 5-HT (PSA = 59.14 Å^2). If passive diffusion and intracellular accumulation of pCA are taken into account, this model recapitulates all pCA mediated currents. Because there is considerable passive pCA flux through membranes, pCA can accumulate in the cell at a much faster rate than 5-HT. If pCA is removed from the external solution, the cell serves as a reservoir. This allows for a continuous outward leak of pCA, which results in concentrations sufficient to trigger pCA-induced currents. This analysis also explains the persistent current observed in *Xenopus laevis* oocytes. The large size of oocytes provides a large intracellular reservoir. Accordingly, upon removal of pCA from the external solution, there is a long-lasting diffusion of pCA into the extracellular medium. Despite continuous superfusion, the unstirred layer of fluid above the cell surface suffices to inhibit immediate removal of pCA (Hille, 1977). Passive cytoplasmic accumulation of pCA also accounts for the pronounced current inhibition in the presence of high external pCA concentrations (Figures 2A, 4B). Consistent with our model [(Schicker *et al.*, 2011); see also Figure 7A], occupation of the inward-facing conformation with a transported ligand should block the transport-associated current by forcing the transporter into the T$_I$S state (Figure 7) (Adams and DeFelice, 2003; Erreger *et al.*, 2008). The resulting rapid rise in internal pCA was detected in HEK293 cells due to the fast solution exchange rate achieved by our superfusion device. At high pCA concentrations, the inhibition occurred with a delay (compare with Figure 4A). It was preceded by a short-lasting current activation (corresponding to concomitant inward transport of pCA by SERT). In our model, the current decay is due to pCA entering the cytoplasm where it competes with K$^+$ for the transporter and thereby inhibits the K$^+$-dependent current.

The molecular stent hypothesis implies that amphetamine binding causes an arrest of the transport cycle, because once the transporter converts from the outward facing to the inward-facing conformation, amphetamines are proposed to stabilize a channel-like mode by binding to a site at the internal gate. Consequently, as long as the amphetamine is bound, the transporter would not undergo a transition to the outward facing conformation (T$_I$K to T$_O$K in our model). However, this transition is facilitated by antiport of K$^+$ (Rudnick and Nelson, 1978; Nelson and Rudnick, 1979). Moreover, we find that intracellular K$^+$ is required for pCA to induce persistent SERT currents (Figure 4A vs. Figure 5), strongly suggesting that these currents, like steady-state 5-HT currents (Schicker *et al.*, 2011), are properties of a transporter intermediate from which substrate (pCA) has already dissociated. This conclusion is in direct opposition to the molecular stent hypothesis, which assumes that amphetamine-induced currents are carried by an intermediate to which amphetamine remains bound.

The present study examined pCA action on SERT. DeFelice and coworkers proposed their hypothesis based on observations in DAT (Rodriguez-Menchaca *et al.*, 2012). Therefore, we also assessed the action of (S+)amphetamine on DAT in HEK293 cells. When we recorded (S+)amphetamine-induced currents we found no evidence for the presence of a persistent current (see Supporting Information Figure S1). Conversely, we observed currents that resembled those from SERT challenged with pCA, suggesting that our conclusions can be extended to DAT.

In the model presented above, we assumed that 5-HT, pCA and MDMA interact with SERT in an identical manner. We are aware that this is an oversimplification because substrates and various amphetamines differ in their affinities for SERT; in addition and more importantly, structure-activity relations indicate that modest structural changes affect the capacity of substituted amphetamines to act as releasers and/or competitive inhibitors of uptake (Rothman and Baumann, 2003). This indicates that the compounds differ in their affinities for the conformational states through which SERT proceeds during the transport cycle (i.e. outward facing, occluded and inward-facing conformation). In our opinion, this does not limit the validity of the model: it provides a framework for refining our understanding on how amphetamine and its congeners elicit their effects on SERT. Finally, the model can be extended to the other monoamine transporters and thus allow for defining how amphetamines discriminate between the three closely related transporters.

Acknowledgements

Conflict of interest

The authors of this article have no conflict of interest.

References

Adams SV, DeFelice LJ (2003). Ionic currents in the human serotonin transporter reveal inconsistencies in the alternating access hypothesis. Biophys J 85: 1548–1559.

Baldwin RL (2013). The new view of hydrophobic free energy. FEBS Lett 587: 1062–1066.

Baumann MH, Ayestas MA, Partilla JS, Sink JR, Shulgin AT, Daley PF et al. (2012). The designer methcathinone analogs, mephedrone and methylone, are substrates for monoamine transporters in brain tissue. Neuropsychopharmacology 37: 1192–1203.

Boehm S (1999). ATP stimulates sympathetic transmitter release via presynaptic P2X purinoceptors. J Neurosci 19: 737–746.

Bulling S, Schicker K, Zhang Y-W, Steinkellner T, Stockner T, Gruber C et al. (2012). The mechanistic basis for noncompetitive ibogaine inhibition of serotonin and dopamine transporters. J Biol Chem 287: 18524–18534.

Erreger K, Grewer C, Javitch JA, Galli A (2008). Currents in response to rapid concentration jumps of amphetamine uncover novel aspects of human dopamine transporter function. J Neurosci 28: 976–989.

Fischer JF, Cho AK (1979). Chemical release of dopamine from striatal homogenates: evidence for an exchange diffusion model. J Pharmacol Exp Ther 208: 203–209.

Fog JU, Khoshbouei H, Holy M, Owens WA, Vaegter CB, Sen N et al. (2006). Calmodulin kinase II interacts with the dopamine transporter C terminus to regulate amphetamine-induced reverse transport. Neuron 51: 417–429.

Gnegy ME (2003). The effect of phosphorylation on amphetamine-mediated outward transport. Eur J Pharmacol 479: 83–91.

Gobbi M, Funicello M, Gerstbrein K, Holy M, Moya PR, Sotomayor R et al. (2008). N,N-dimethyl-thioamphetamine and methyl-thioamphetamine, two non-neurotoxic substrates of 5-HT transporters, have scant in vitro efficacy for the induction of transporter-mediated 5-HT release and currents. J Neurochem 105: 1770–1780.

Hilber B, Scholze P, Dorostkar MM, Sandtner W, Holy M, Boehm S et al. (2005). Serotonin-transporter mediated efflux: a pharmacological analysis of amphetamines and non-amphetamines. Neuropharmacology 49: 811–819.

Hille B (1977). The pH-dependent rate of action of local anesthetics on the node of Ranvier. J Gen Physiol 69: 475–496.

Kahlig KM, Binda F, Khoshbouei H, Blakely RD, McMahon DG, Javitch J et al. (2005). Amphetamine induces dopamine efflux through a dopamine transporter channel. Proc Natl Acad Sci U S A 102: 3495–3500.

Kristensen AS, Andersen J, Jørgensen TN, Sørensen L, Eriksen J, Loland CJ et al. (2011). SLC6 neurotransmitter transporters: structure, function, and regulation. Pharmacol Rev 63: 585–640.

Laeuger P (1991). Electrogenic Ion Pumps. Sinauer Associates Inc: Sunderland, MA.

Lin F, Lester HA, Mager S (1996). Single-channel currents produced by the serotonin transporter and analysis of a mutation affecting ion permeation. Biophys J 71: 3126–3135.

Mager S, Min C, Henry DJ, Chavkin C, Hoffman BJ, Davidson N et al. (1994). Conducting states of a mammalian serotonin transporter. Neuron 12: 845–859.

Nelson PJ, Rudnick G (1979). Coupling between platelet 5-hydroxytryptamine and potassium transport. J Biol Chem 254: 10084–10089.

Petersen CI, DeFelice LJ (1999). Ionic interactions in the Drosophila serotonin transporter identify it as a serotonin channel. Nat Neurosci 2: 605–610.

Quick MW (2003). Regulating the conducting states of a mammalian serotonin transporter. Neuron 40: 537–549.

Reynolds JA, Gilbert DB, Tanford C (1974). Empirical correlation between hydrophobic free energy and aqueous cavity surface area. Proc Natl Acad Sci U S A 71: 2925–2927.

Rodriguez-Menchaca AA, Solis E, Cameron K, De Felice LJ (2012). S(+)amphetamine induces a persistent leak in the human dopamine transporter: molecular stent hypothesis. Br J Pharmacol 165: 2749–2757.

Rothman RB, Baumann MH (2003). Monoamine transporters and psychostimulant drugs. Eur J Pharmacol 479: 23–40.

Rudnick G, Nelson PJ (1978). Platelet 5-hydroxytryptamine transport, an electroneutral mechanism coupled to potassium. Biochemistry 17: 4739–4742.

Rudnick G, Wall SC (1992). p-Chloroamphetamine induces serotonin release through serotonin transporters. Biochemistry 31: 6710–6718.

Schicker K, Uzelac Z, Gesmonde J, Bulling S, Stockner T, Freissmuth M et al. (2011). A unifying concept of serotonin transporter associated currents. J Biol Chem 287: 438–445.

Schmidt H, Jirstrand M (2006). Systems Biology Toolbox for MATLAB: a computational platform for research in systems biology. Bioinformatics 22: 514–515.

Seidel S, Singer EA, Just H, Farhan H, Scholze P, Kudlacek O et al. (2005). Amphetamines take two to tango: an oligomer-based counter-transport model of neurotransmitter transport explores the amphetamine action. Mol Pharmacol 67: 140–151.

Sitte HH, Freissmuth M (2010). The reverse operation of Na(+)/Cl(-)-coupled neurotransmitter transporters-why amphetamines take two to tango. J Neurochem 112: 340–355.

Sitte HH, Huck S, Reither H, Boehm S, Singer EA, Pifl C (1998). Carrier-mediated release, transport rates, and charge transfer induced by amphetamine, tyramine, and dopamine in mammalian cells transfected with the human dopamine transporter. J Neurochem 71: 1289–1297.

Sitte HH, Hiptmair B, Zwach J, Pifl C, Singer EA, Scholze P (2001). Quantitative analysis of inward and outward transport rates in cells

stably expressing the cloned human serotonin transporter: inconsistencies with the hypothesis of facilitated exchange diffusion. Mol Pharmacol 59: 1129–1137.

Sonders MS, Zhu SJ, Zahniser NR, Kavanaugh MP, Amara SG (1997). Multiple ionic conductances of the human dopamine transporter: the actions of dopamine and psychostimulants. J Neurosci 17: 960–974.

Steinkellner T, Yang J-W, Montgomery TR, Chen W-Q, Winkler M-T, Sucic S et al. (2012). Ca(2+)/calmodulin-dependent protein kinase IIα (αCaMKII) controls the activity of the dopamine transporter: implications for Angelman syndrome. J Biol Chem 287: 29627–29635.

Sucic S, Dallinger S, Zdrazil B, Weissensteiner R, Jørgensen TN, Holy M et al. (2010). The N terminus of monoamine transporters is a lever required for the action of amphetamines. J Biol Chem 285: 10924–10938.

Sulzer D, Maidment NT, Rayport S (1993). Amphetamine and other weak bases act to promote reverse transport of dopamine in ventral midbrain neurons. J Neurochem 60: 527–535.

Sulzer D, Chen TK, Lau YY, Kristensen H, Rayport S, Ewing A (1995). Amphetamine redistributes dopamine from synaptic vesicles to the cytosol and promotes reverse transport. J Neurosci 15: 4102–4108.

Supporting Information

Additional Supporting Information may be found in the online version of this article at the publisher's web-site:

http://dx.doi.org/10.1111/bph.12520

Figure S1 A representative current trace recorded from DAT expressed in a HEK293 cell. The cell was clamped to −70 mV utilizing the whole cell patch clamp technique. The cell was challenged with 100 μM (S+)-amphetamine for 5 s. Upon wash-out of (S+)-amphetamine the current decayed slowly to initial values. However, a persistent current was not observed. **Scheme S1** Cell modelled as a sphere.